Microscopic Origin of Heisenberg and Non-Heisenberg Exchange Interactions in Ferromagnetic bcc Fe

Y. O. Kvashnin,[1] R. Cardias,[2] A. Szilva,[1] I. Di Marco,[1] M. I. Katsnelson,[3,4] A. I. Lichtenstein,[4,5] L. Nordström,[1] A. B. Klautau,[2] and O. Eriksson[1]

[1]Department of Physics and Astronomy, Division of Materials Theory, Uppsala University, Box 516, SE-75120 Uppsala, Sweden
[2]Faculdade de Fisica, Universidade Federal do Para, Belem, Pará 66075-110, Brazil
[3]Radboud University of Nijmegen, Institute for Molecules and Materials, Heijendaalseweg 135, 6525 AJ Nijmegen, Netherlands
[4]Theoretical Physics and Applied Mathematics Department, Ural Federal University, Mira Street 19, 620002 Ekaterinburg, Russia
[5]Institute of Theoretical Physics, University of Hamburg, Jungiusstrasse 9, 20355 Hamburg, Germany

(Received 8 October 2015; published 27 May 2016)

By means of first principles calculations, we investigate the nature of exchange coupling in ferromagnetic bcc Fe on a microscopic level. Analyzing the basic electronic structure reveals a drastic difference between the $3d$ orbitals of E_g and T_{2g} symmetries. The latter ones define the shape of the Fermi surface, while the former ones form weakly interacting impurity levels. We demonstrate that, as a result of this, in Fe the T_{2g} orbitals participate in exchange interactions, which are only weakly dependent on the configuration of the spin moments and thus can be classified as Heisenberg-like. These couplings are shown to be driven by Fermi surface nesting. In contrast, for the E_g states, the Heisenberg picture breaks down since the corresponding contribution to the exchange interactions is shown to strongly depend on the reference state they are extracted from. Our analysis of the nearest-neighbor coupling indicates that the interactions among E_g states are mainly proportional to the corresponding hopping integral and thus can be attributed to be of double-exchange origin. By making a comparison to other magnetic transition metals, we put the results of bcc Fe into context and argue that iron has a unique behavior when it comes to magnetic exchange interactions.

DOI: 10.1103/PhysRevLett.116.217202

Iron is one of the most abundant elements in the Universe. Its elemental phase has several polymorphs which are composed in a rather complex phase diagram [1]. Among these phases, most stable crystal structure at ambient conditions is a body-centered cubic (bcc or α) one. The bcc phase is ferromagnetic (FM) up to the critical temperature (T_c) of 1045 K. Above the Curie point, the bcc structure is preserved in a certain temperature range before it undergoes a transition to the fcc phase. This fact implies that the local magnetic moments exist in the paramagnetic (PM) phase, where a strong short-range magnetic order was proposed [2]. Moreover, the further increase of temperature leads first to the stability of a fcc (γ) phase and, at even higher temperatures, to the reentrance to another bcc (δ) phase. It is well known that such a peculiar P-T diagram of iron is defined, to a large extent, by the magnetic degrees of freedom [3,4]. Thus, the contribution of the magnetic fluctuations to the free energy is important and the information about the interatomic exchange parameters is vital. This is also the case, when it comes to the stability of Fe-based alloys and steels [5]. Other areas of materials science where the exchange interaction between Fe atoms becomes important are, e.g., magnetocalorics (e.g., in Fe_2P-based alloys [6]) and ultrafast magnetization dynamics [7].

Both the T_c and the magnon excitation spectra of iron at low temperatures can be well described by means of the Heisenberg Hamiltonian (HH), parametrized by *ab initio* calculations [8–16]. However, in several works [17–21] it was argued that, in order to describe a large palette of magnetic states, higher-order (biquadratic) exchange interactions have to be taken into account. The results of the self-consistent spin spiral calculations also indicate that the magnitude of the magnetic moment in bcc Fe can differ by almost 30% in various configurations [22,23], which, in principle, disagrees with the assumptions of the Heisenberg picture.

Correlation effects are known to be important for bcc Fe at finite temperatures, as was shown in Ref. [24] by means of density functional theory plus dynamical mean field theory (DFT + DMFT) calculations. It has been suggested that electron correlations play a role, and from a qualitative analysis of the electronic structure that the E_g electrons in iron are much more correlated than the T_{2g} ones [25]. This statement was quantitatively investigated, using DFT + DMFT calculations for the PM phase of bcc Fe [26]. According to Ref. [26], the E_g and T_{2g} states have to be analyzed separately in this system. Both types of orbitals were found to contribute equally to the formation of the local moment in its PM phase. Recently, Igoshev *et al.* [27] has presented an analysis of the orbital-resolved dynamical susceptibility again using DFT + DMFT formalism. The E_g-T_{2g} exchange interactions were suggested to play the main role in the magnetic couplings.

In this work we perform an orbital-by-orbital analysis on the magnetic interactions in the FM bcc phase, using DFT and DFT + DMFT, and make an attempt to classify them and associate them with the well-known textbook exchange mechanisms. Surprisingly, we find that there is a strong antiferromagnetic (AFM) component to the nearest-neighbor (NN) exchange interaction (J_1) for the states of T_{2g} character. This is caused by the Ruderman-Kittel-Kasuya-Yosida (RKKY)-type coupling [28,29], governed by the topology of the Fermi surface (FS). In contrast, the E_g states contribute ferromagnetically to the NN coupling with a combination of double exchange (DE) and superexchange. As a consequence, the E_g states give rise to short-range magnetic interactions in bcc Fe, whereas T_{2g} states contribute to longer range couplings, with a pronounced oscillatory behavior.

The calculations were performed with the use of standard DFT techniques by means of either real-space linear muffin-tin orbital (LMTO) method within the atomic sphere approximation [30,31] or a full-potential realization of the LMTO method [32]. We employed the standard local spin density approximation (LSDA) for the exchange-correlation energy throughout the study, but explicitly demonstrate that the inclusion of the many-body correlations within DMFT does not affect the results significantly. The intersite exchange integrals (J_{ij}'s) were extracted by means of the magnetic force theorem (MFT) [10]. Within this approach, the magnetic subsystem is mapped onto a HH of the conventional form (see, e.g., Refs. [8,9]). For some calculations, we have also adopted a recent generalization of the MFT, allowing for treatment of the noncollinear spin structures [17]. In addition to the total value of the J_{ij}, we have computed the individual orbital contributions to each particular coupling (for details, see, e.g., Ref. [33]). The latter ones were grouped according to the representations of the cubic space group, so that each exchange integral is represented as

$$J_{ij} = J_{ij}^{E_g\text{-}E_g} + J_{ij}^{E_g\text{-}T_{2g}} + J_{ij}^{T_{2g}\text{-}T_{2g}}, \tag{1}$$

where, for instance, $J_{ij}^{E_g\text{-}T_{2g}}$ denotes an aggregate strength of the coupling of the E_g orbitals located on the site $i(j)$ interacting with the T_{2g} subset located at the site $j(i)$. For an arbitrary i-j pair, the aforementioned *mixed* couplings are allowed by symmetry even in the $\mathrm{Im}\bar{3}m$ space group. This is so because J_{ij} is an intersite quantity and thus depends on the bonding vector $\mathbf{R_{ij}}$, which, in most cases, locally destroys the full cubic symmetry, hence allowing for mixing between the E_g and T_{2g} orbitals.

In order to put Fe into the perspective of the 3d series, we have calculated NN exchange (J_1) for Cr, Mn, Fe, Co, and Ni in a bcc crystal structure. We chose a common crystal structure since it becomes easier to follow the trends across the series and to build the connection with the filling of

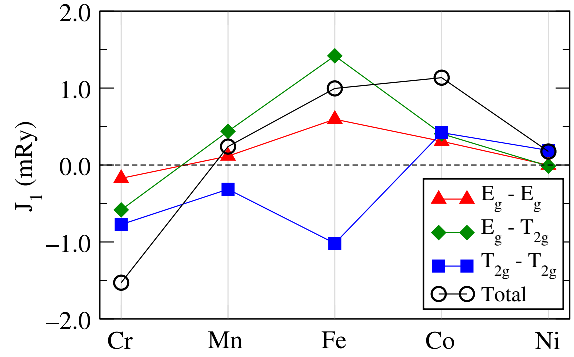

FIG. 1. Orbitally decomposed NN exchange interaction in elemental 3d metals in the bcc structure.

electron states. The results of the total exchange interaction, as well as its symmetry-resolved components, are shown in Fig. 1. One can see that the total values of the NN interaction follow the celebrated Bethe-Slater curve [34] perfectly. However, looking at the decomposition of each coupling to symmetry-resolved contributions reveals a few surprises. Mn and Fe are the only two elements where different orbital couplings are substantially large but, at the same time, have opposite signs. This competition is the most pronounced in Fe, where all three symmetry-resolved contributions have comparable strength, which makes this system special among all 3d metals. Such a strong AFM contribution to the NN coupling is surprising for bcc Fe, which is known as one of the most stable ferromagnetic materials. We also note from Fig. 1 that for Mn the contributions to J_1 compete with each other, and that this element's position at the border between the FM and AFM interaction [35–38] is a consequence of this competition. The data in Fig. 1 highlight the unique interaction of bcc Fe, having an AFM T_{2g}-T_{2g} contribution that dwarfs that of any other 3d element, including the AFM phase of bcc Cr. The net NN interaction of bcc Fe becomes ferromagnetic only due to equally large and positive E_g-E_g and E_g-T_{2g} interactions. Since bcc Fe stands out so much in Fig. 1, most of the discussion in the remainder of this Letter is focused on it.

We continued by performing a set of calculations of the noncollinear exchange by rotating a single Fe moment on an angle θ with respect to a FM background. At each given θ, the J_{ij} parameters were extracted following the recipe given in Ref. [17]. We found that, for any value of θ, the $J_1^{T_{2g}\text{-}T_{2g}}$ is practically independent of the mutual orientation of spins, thus suggesting that the magnetic interaction of these orbitals is well described by the HH. In contrast, the $J_1^{E_g\text{-}E_g}$ and $J_1^{E_g\text{-}T_{2g}}$ contributions become modified, so that for large values of θ they amount to 230% and 150%, respectively, of the $\theta = 0$ values. It has been suggested that this pronounced θ dependence is due to DE [39,40], something we investigate in detail below. However, at this stage we can already conclude that the J_1 coupling in bcc

Fe consists of FM and AFM contributions, having a very different dependence on the spin configuration.

Here, we argue that, in the case of Fe, it is possible to attribute each symmetry-resolved part of the J_1 to different microscopic mechanisms. To carry out such an analysis, one has to start by investigating the orbital-projected density of states (DOS), shown for bcc Fe in the Supplemental Material [41]. What is important from the DOS figure is that the FS is almost entirely formed by the T_{2g} states, which was already pointed out in Ref. [44]. In contrast, as is seen from the DOS, the E_g orbitals form a set of half-filled quasi-impurity states. Such a clear difference is expected to lead to a very pronounced difference concerning the nature of the exchange couplings. For instance, mechanisms associated with details of the FS, like the RKKY-type interaction, are expected to be more pronounced for the T_{2g} states since these states dominate the Fermi surface. Before we continue with this analysis we note that, in order to investigate the influence of electron correlations, we investigated the effective J_{ij}'s extracted from LSDA + DMFT calculation for FM bcc Fe (see the Supplemental Material [41]). We found that the inclusion of dynamical correlations affects, to some extent, the strength of orbital-resolved contributions to the exchange couplings, but it does not modify their sign or relative strength. Thus, the conclusions drawn from the results of the LSDA calculations remain valid even when a more accurate (but complicated) description of the electronic structure is employed.

To address the nature of the magnetic exchange further, we have analyzed the long-range magnetic interactions in bcc Fe along several high-symmetry directions. It was found that T_{2g}-T_{2g} interactions indeed have pronounced RKKY-type oscillations, particularly along the (111) direction, i.e., the direction along the NN bonding vector. For this specific direction, we show in Fig. 2 $J_{ij}R_{ij}^3$ as a function of the intersite distance R_{ij}, resolved into different symmetry components. One can see that the E_g-E_g and E_g-T_{2g} contributions decay rather quickly and are already negligible for the third NN along this path. The T_{2g}-T_{2g} part, on the contrary, is extremely long-range and gives the main contribution to the total coupling at large distances. Thus, it is clear that the T_{2g} electrons are responsible for a RKKY-type exchange in bcc Fe.

Furthermore, we analyzed the period of the observed oscillations with an emphasis on the features of the FS. The exchange couplings along this direction are primarily defined by the excitations, carrying the momenta parallel to the high-symmetry line Λ (i.e., along the Γ-P direction). In fact, in this part of the Brillouin zone, the FS topology is trivial and is characterized by the presence of one electron pocket per spin channel [11,44]. Moreover, the orbitally projected band structures suggest that these bands have a pure T_{2g} character (see the Supplemental Material [41]),

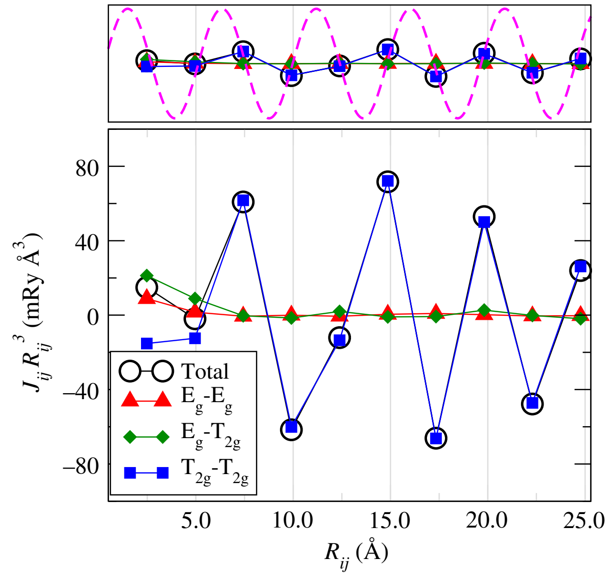

FIG. 2. (Bottom panel) $J_{ij}R_{ij}^3$ with the neighbors selected to lie along the (111) direction in bcc Fe. R_{ij} is the intersite distance. (Top panel) The same data plotted together with an analytical function $y = A_0 \sin(1.3R_{ij} + \phi_0)$ (the dashed curve), whose period was obtained from the FS analysis. A_0 and ϕ_0 were adjusted to give the best agreement with the DFT results.

which is in line with our conclusions about the origin of the RKKY-type oscillations. We have analyzed in detail the band structure and have obtained the following values for the Fermi wave vectors: $k_F^{\downarrow} = 0.94$ Å^{-1} and $k_F^{\uparrow} = 0.36$ Å^{-1}. The period of the RKKY-type oscillations is expected to be defined by the calliper vector [14], i.e., $k_F^{\uparrow} + k_F^{\downarrow} \approx 1.30$ Å^{-1}. We fitted the computed oscillatory exchange interactions of Fig. 2 with a sine function of the period, extracted above. The result is shown in the top panel of Fig. 2. One can see that the analytical results nicely reproduce the outcomes of our numerical calculations. In the Supplemental Material [41], we also demonstrate that the shift of the E_F leads to the modification of $k_F^{\uparrow(\downarrow)}$, which is consistent with the change of the period of RKKY oscillations. This represents strong evidence that the T_{2g} states primarily participate in the Heiseberg-like exchange interactions, driven by a RKKY-type mechanism.

In contrast, the E_g electrons are involved in other types of magnetic interactions. In order to shed light on their nature, we have performed an analysis based on the tight-binding picture. The main quantity in this theory is the intersite hopping integral (t). The hopping integral between two $3d$ orbitals ($l = 2$) located at different sites is expected to scale as d^{-5}, where d is the distance between the sites (see, e.g., Ref. [45]). Note that this relation can also be derived directly from the LMTO formalism [46] and is valid for modifications of the lattice parameter within 5% to 10% [47,48]. Typically, different contributions to the exchange couplings scale with different powers of t. For instance, the FM DE is proportional to t ($\propto d^{-5}$), while the AFM superexchange has a t^2 dependence ($\propto d^{-10}$). In order to identify their relative contributions, we have performed DFT calculations for bcc Fe for different volumes around the equilibrium. Based on the aforementioned arguments, we performed the fittings of individual orbital contributions to J_1 using the following expression:

$$J_1 = \alpha d^{-5} - \beta d^{-10}, \tag{2}$$

where α and β are the fitting parameters. The results of the *ab initio* calculations along with the fitted functions are shown in Fig. 3. The E_g-E_g and E_g-T_{2g} components of the J_1 could both be successfully fitted. The obtained values of α and β clearly indicate that the FM DE contribution strongly prevails over the AFM part. Moreover, one can see the crucial role of the E_g-T_{2g} interactions on the ferromagnetism of iron: it provides the dominant FM component of the J_1 coupling. This observation is in line with a recent study by Igoshev *et al.* [27], who analyzed the paramagnetic susceptibility in bcc Fe and also emphasized an importance of the mixed E_g-T_{2g} interactions for the formation of the local moment. The results shown in Fig. 3 show that the primary contribution to $J_1^{E_g\text{-}E_g}$ and $J_1^{E_g\text{-}T_{2g}}$ is proportional to the first power of the effective hopping integral t. Moreover, we have shown above that the NN E_g-E_g and E_g-T_{2g} interactions have a pronounced θ dependence, which implies their non-Heisenberg origin. This allows us to conclude that these interactions are not primarily dominated by biquadratic interactions. We draw this conclusion because biquadratic exchange interactions are proportional to higher powers of t (see, e.g., Ref. [49]). Thus, bringing all the evidence together, we conclude that

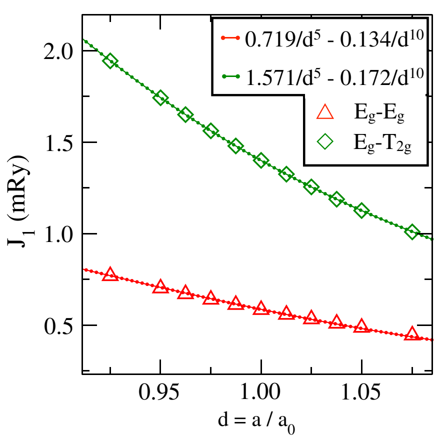

FIG. 3. Distance dependence of the $J_1^{E_g\text{-}E_g}$ and $J_1^{E_g\text{-}T_{2g}}$ interactions in bcc Fe. a_0 corresponds to the equilibrium lattice constant (2.86 Å). To facilitate the analysis, the magnetic moment was constrained to the value obtained self-consistently for $a = a_0$, which is 2.2 μ_B.

the DE mechanism is the main source of the NN E_g-E_g and E_g-T_{2g} interactions in bcc Fe.

We demonstrate here that there is a strong competition between FM and AFM contributions to the NN exchange coupling coming from different $3d$ orbitals in the bcc phase of Mn and, particularly, Fe. It is shown numerically that the exchange coupling between the T_{2g} orbitals is relatively independent of the mutual orientation of the spins, thus suggesting their Heisenberg-like nature. This conclusion is supported by the analysis of the long-range exchange couplings along the NN direction. The period of RKKY-type oscillations was shown to be related to the nesting of the FS, which is dominated by contributions from the T_{2g} states. The E_g electrons, on the contrary, produce relatively short-range interactions with a substantial non-Heisenberg behavior. Our analysis demonstrates that the interactions between the E_g states can be attributed to a double-exchange mechanism.

In the last 15 years enormous progress has been achieved in the development of experimental techniques for measuring magnon excitations. For instance, it was shown that, by means of spin-polarized electron energy loss spectroscopy [50], it is possible to identify the atomic contributions to certain spin wave modes [51]. A sufficient theoretical foundation as well as an improvement of experimental resolution opened the way for resonant inelastic x-ray scattering to be used as a tool to probe magnon excitations [52]. The latter method also allows us to control the polarization of the E field of the photon beam and, therefore, opens the possibility for selecting states of a particular symmetry in the excitation process. In this Letter we suggest that the primary role in long-range magnetic interactions is played by the T_{2g} electrons, which have a strong AFM NN coupling. Given the pace of advancement of the above-mentioned experimental techniques, such predictions will hopefully soon get their experimental verification.

Y. K. is grateful to P. Bruno (ESRF) for the useful discussions. R. C. and A. B. K. acknowledge financial support from CAPES and CNPq, Brazil. M. I. K. acknowledges the financial support from European Research Council (ERC) Advanced Grant No. 338957 FEMTO/NANO. O. E. acknowledges the support from Swedish Research Council (VR), eSSENCE, and the KAW Foundation (Grants No. 2012.0031 and No. 2013.0020). The authors acknowledge the computational resources provided by the Swedish National Infrastructure for Computing (SNIC) and Uppsala Multidisciplinary Center for Advanced Computational Science (UPPMAX).

[1] H. M. Strong, R. E. Tuft, and R. E. Hanneman, Metall. Trans. **4**, 2657 (1973); R. Boehler, Geophys. Res. Lett. **13**, 1153 (1986).

[2] X. Tao, D. P. Landau, T. C. Schulthess, and G. M. Stocks, Phys. Rev. Lett. **95**, 087207 (2005).

[3] C. Zener, in *Phase Stability in Metals and Alloys*, edited by P. S. Rudman, J. Sringer, and R. I. Jaffee (McGraw-Hill, New-York, 1967), p. 25.

[4] H. Hasegawa and D. G. Pettifor, Phys. Rev. Lett. **50**, 130 (1983).

[5] J. Neugebauer and T. Hickel, WIREs Comput. Mol. Sci. **3**, 438 (2013).

[6] E. K. Delczeg-Czirjak, L. Bergqvist, O. Eriksson, Z. Gercsi, P. Nordblad, L. Szunyogh, B. Johansson, and L. Vitos, Phys. Rev. B **86**, 045126 (2012).

[7] R. Chimata, A. Bergman, L. Bergqvist, B. Sanyal, and O. Eriksson, Phys. Rev. Lett. **109**, 157201 (2012).

[8] J. Kubler, *Theory of Itinerant Electron Magnetism* (Oxford University Press, New York, 2009).

[9] P. Mohn, *Magnetism in the Solid State* (Springer, New York, 2003).

[10] A. I. Liechtenstein, M. I. Katsnelson, V. P. Antropov, and V. A. Gubanov, J. Magn. Magn. Mater. **67**, 65 (1987).

[11] S. V. Halilov, H. Eschrig, A. Y. Perlov, and P. M. Oppeneer, Phys. Rev. B **58**, 293 (1998).

[12] V. P. Antropov, B. N. Harmon, and A. N. Smirnov, J. Magn. Magn. Mater. **200**, 148 (1999).

[13] M. I. Katsnelson and A. I. Lichtenstein, Phys. Rev. B **61**, 8906 (2000).

[14] M. Pajda, J. Kudrnovský, I. Turek, V. Drchal, and P. Bruno, Phys. Rev. B **64**, 174402 (2001).

[15] Y. O. Kvashnin, O. Grånäs, I. Di Marco, M. I. Katsnelson, A. I. Lichtenstein, and O. Eriksson, Phys. Rev. B **91**, 125133 (2015).

[16] C. Etz, L. Bergqvist, A. Bergman, A. Taroni, and O. Eriksson, J. Phys. Condens. Matter **27**, 243202 (2015).

[17] A. Szilva, M. Costa, A. Bergman, L. Szunyogh, L. Nordstrom, and O. Eriksson, Phys. Rev. Lett. **111**, 127204 (2013).

[18] R. Singer, F. Dietermann, and M. Fähnle, Phys. Rev. Lett. **107**, 017204 (2011).

[19] S.A. Turzhevskii, A.I. Lichtenstein, and M.I. Katsnelson, Fiz. Tverd. Tela **32**, 1952 (1990) [Sov. Phys. Solid State **32**, 1138 (1990)].

[20] M. U. Luchini and V. Heine, Europhys. Lett. **14**, 609 (1991).

[21] D. Böttcher, A. Ernst, and J. Henk, J. Magn. Magn. Mater. **324**, 610 (2012).

[22] S. Shallcross, A. E. Kissavos, V. Meded, and A. V. Ruban, Phys. Rev. B **72**, 104437 (2005).

[23] S. V. Okatov, Yu. N. Gornostyrev, A. I. Lichtenstein, and M. I. Katsnelson, Phys. Rev. B **84**, 214422 (2011).

[24] A. I. Lichtenstein, M. I. Katsnelson, and G. Kotliar, Phys. Rev. Lett. **87**, 067205 (2001).

[25] V. Yu. Irkhin, M. I. Katsnelson, and A. V. Trefilov, J. Phys. Condens. Matter **5**, 8763 (1993).

[26] A. A. Katanin, A. I. Poteryaev, A. V. Efremov, A. O. Shorikov, S. L. Skornyakov, M. A. Korotin, and V. I. Anisimov, Phys. Rev. B **81**, 045117 (2010).

[27] P. A. Igoshev, A. V. Efremov, and A. A. Katanin, Phys. Rev. B **91**, 195123 (2015).

[28] M. A. Ruderman and C. Kittel, Phys. Rev. **96**, 99 (1954).

[29] Here, we mention that the original formulation of the RKKY mechanism implies an interaction of local magnetic moments via sea of the conduction electrons. In the case of itinerant ferromagnets, the $3d$ electrons are responsible for formation of both the magnetic moment and the Fermi surface. We refer the reader to Ref. [14] for more details.

[30] P. R. Peduto, S. Frota-Pessoa, and M. S. Methfessel, Phys. Rev. B **44**, 13283 (1991).

[31] S. Frota-Pessoa, Phys. Rev. B **46**, 14570 (1992).

[32] J. M. Wills, O. Eriksson, M. Alouani, and D. L. Price, in *Electronic Structure and Physical Properties of Solids*, Lecture Notes in Physics Vol. 535, edited by H. Dreysse (Springer, Berlin, 2000), p. 148.

[33] Dm. M. Korotin, V. V. Mazurenko, V. I. Anisimov, and S. V. Streltsov, Phys. Rev. B **91**, 224405 (2015).

[34] J. C. Slater, Phys. Rev. **35**, 509 (1930); **36**, 57 (1930); A. Sommerfeld and H. Bethe, in *Handbuch der Physik*, Vol. 24, edited by H. Geiger and K. Scheel (Springer, Berlin, 1933), Part 2, p. 595.

[35] D. Hobbs, J. Hafner, and D. Spisák, Phys. Rev. B **68**, 014407 (2003); J. Hafner and D. Hobbs, Phys. Rev. B **68**, 014408 (2003).

[36] P. Bobadova-Parvanova, K. A. Jackson, S. Srinivas, and M. Horoi, J. Chem. Phys. **122**, 014310 (2005).

[37] M. Friák and M. Šob, Phys. Rev. B **77**, 174117 (2008).

[38] G. Steinle-Neumann, R. E. Cohen, and L. Stixrude, J. Phys. Condens. Matter **16**, S1109 (2004); G. Steinle-Neumann, L. Stixrude, and R. E. Cohen, Proc. Natl. Acad. Sci. U.S.A. **101**, 33 (2004).

[39] P. W. Anderson and H. Hasegawa, Phys. Rev. **100**, 675 (1955).

[40] M. I. Auslender and M. I. Katsnelson, Theor. Math. Phys. **51**, 601 (1982).

[41] See Supplemental Material at http://link.aps.org/supplemental/10.1103/PhysRevLett.116.217202, which includes Refs. [42,43], for the additional results of the calculations.

[42] A. Grechnev, I. Di Marco, M. I. Katsnelson, A. I. Lichtenstein, J. Wills, and O. Eriksson, Phys. Rev. B **76**, 035107 (2007).

[43] M. I. Katsnelson and A. I. Lichtenstein, Eur. Phys. J. B **30**, 9 (2002).

[44] J. Schäfer, M. Hoinkis, E. Rotenberg, P. Blaha, and R. Claessen, Phys. Rev. B **72**, 155115 (2005).

[45] W. A. Harrison, *Electronic Structure and the Properties of Solids: The Physics of the Chemical Bond* (Dover, New York, 1979).

[46] O. K. Andersen, W. Klose, and H. Nohl, Phys. Rev. B **17**, 1209 (1978).

[47] J. D. Shore and D. A. Papaconstantopoulos, Phys. Rev. B **35**, 1122 (1987).

[48] M. H. F. Sluiter and P. P. Singh, Phys. Rev. B **49**, 10918 (1994).

[49] F. Mila and F.-C. Zhang, Eur. Phys. J. B **16**, 7 (2000).

[50] R. Vollmer, M. Etzkorn, P. S. Anil Kumar, H. Ibach, and J. Kirschner, Phys. Rev. Lett. **91**, 147201 (2003).

[51] Kh. Zakeri, T.-H. Chuang, A. Ernst, L. M. Sandratskii, P. Buczek, H. J. Qin, Y. Zhang, and J. Kirschner, Nat. Nanotechnol. **8**, 853 (2013).

[52] L. Braicovich *et al.*, Phys. Rev. Lett. **104**, 077002 (2010).